JMEPEG (2009) 18:414–419
DOI: 10.1007/s11665-008-9296-3

1059-9495/$19.00

Mechanical Properties and Thermal Shock Resistance of Al_2O_3-TiC-Co Composites

Rui-xia Shi, Jia Li, Dong-zhi Wang, and Yan-sheng Yin

(Submitted December 4, 2007; in revised form June 29, 2008)

Ductile cobalt was introduced into Al_2O_3-TiC (AT) composites by using a chemical deposition method to improve toughness and resistance to thermal shock. The mixture of Co-coated Al_2O_3 and TiC powders was hot-pressed into an Al_2O_3-TiC-Co (ATC) composite. The flexure strength and fracture toughness of the ATC composites have been improved considerably, compared with AT and Al_2O_3. The fracture surface of ATC shows a large proportion of transgranular cracks with some intergranular type, unlike the intergranular fracture modes of AT and Al_2O_3. The thermal shock properties of the composites were evaluated by water quenching technique and compared with the traditional AT and Al_2O_3. The composites containing only 3.96 vol.% cobalt exhibited higher critical temperature difference and retained flexure strength. The SEM examination of the fracture surfaces of the ATC composites after single thermal cycle showed that voids increased in number and size, and most isolated voids coalesced with increasing temperature difference, which caused the density and strength to decrease. The ATC composite is less sensitive to repeated thermal shock than the AT composite.

Keywords Al_2O_3-TiC-Co, composites, mechanical properties, thermal shock resistance

1. Introduction

Alumina ceramics, one of the most successful engineering ceramics, have great potential to be used in many special applications where low density, high stiffness, high hardness, chemical inertness, and good high-temperature properties are required (Ref 1). However, their poor mechanical properties, especially fracture toughness, make them difficult to withstand severe conditions applied, for example, in the field of high-speed cutting tools. From the viewpoint of multiphase ceramics, the flexure strength and fracture toughness of the alumina matrix materials can be enhanced by incorporating second phase particles, such as Co, TiC, TiN, TiB_2, (W,Ti)C, Ti(C,N), ZrO_2, SiCp (Ref 2-6). Al_2O_3-TiC (AT) composites have been widely utilized in various engineering fields due to their advantages such as higher hardness, strength, chemical stability, and excellent wear resistance relative to Al_2O_3 ceramics. In many applications, the Al_2O_3-TiC composites are often exposed to rapid temperature changes, which might cause severe thermal stress and thermal shock damage due to their lower strength and thermal properties. Therefore, how to improve the thermal shock resistance of Al_2O_3-TiC composites has been an important issue in their structural applications.

Rui-xia Shi, Jia Li, and **Dong-zhi Wang**, School of Materials Science and Engineering, University of Jinan, Jinan, Shandong 250022, China; and **Rui-xia Shi** and **Yan-sheng Yin**, School of Materials Science and Engineering, Ocean University of China, Qingdao, Shandong 266100, China. Contact e-mail: mse_shirx@ujn.edu.cn.

Incorporation of a ductile phase into a brittle ceramic matrix has been proved to be an effective mechanism to toughen the ceramic because the existence of the ductile phase can dissipate the energy of crack initiation and propagation through plastic deformation, thus making a larger contribution to the increment of toughness of brittle ceramic materials. Cobalt, a common cohesive phase in cermets, possesses a unique set of physical properties and favorable wettability to TiC. In the present paper, a kind of novel Al_2O_3-TiC-Co (ATC) composites was prepared from cobalt-coated ceramic powders by a newly developed coating technique, which was expected to improve the mechanical and thermal shock performance (Ref 7). Due to the presence of cobalt film, the ATC composites exhibit better mechanical properties and thermal shock resistance than the AT composites and Al_2O_3.

2. Experimental Procedures

The Al_2O_3 (average particle size ~40 nm) and TiC (average particle size ~130 nm) powders were coated with cobalt film (cobalt content about 3.96 vol.%) by using electroless method. The coated powders and Al_2O_3-TiC powders with the weight ratio of 7:3 (Al_2O_3:TiC) (provided by Ningbo Lingri Surface Engineering Co. Ltd., Zhejiang, China) were then homogenized by ultrasonic dispersion as the starting powders, and were hot-pressed in vacuum at 1650 °C for 30 min under 30 MPa. The sinters were cut into bars of dimensions $3 \times 4 \times 36$ mm^3 and $2 \times 4 \times 36$ mm^3, respectively, ground, and polished to 1 μm finish. The specimen edges were slightly beveled on 1200-grit emery paper to decrease the effect of edge cracks and to remove notches introduced in the course of machining.

The thermal shock resistance of composites was evaluated by water quenching technique. The test bars were heated to desired temperatures for 30 min in a drop-bottom furnace and then quenched into a container of water at 25 °C. The thermal

quenching of single thermal shock specimen was conducted at initial temperatures ranging from 25 to 1025 °C, which corresponded to thermal shock temperature differences of 0 to 1000 °C. Repeated thermal shock tests, up to 20 cycles, were carried out at a temperature difference, ΔT, of 400 °C.

Five samples were tested for each temperature difference. The shocked bars were dried before their retained strength was measured at room temperature. The flexure strength of specimens was measured by three-point bending test ($3 \times 4 \times 36$ mm^3 in dimensions), with a span length of 20 mm and a crosshead speed of 0.5 mm/min. The fracture toughness tests were performed by the single edge notched beam (SENB) method ($2 \times 4 \times 36$ mm^3 in dimensions) at a loading rate of 0.5 mm/min with a notch 2 mm in depth and 0.25 mm in width and a span of 20 mm. The densities of the sintered samples were measured using Archimedes principle. The phase composition after thermal shock was identified on the fracture surface using x-ray diffraction (XRD) (*D*/max-rA, Japan) with Cu K_α radiation. The fracture surfaces were investigated using a scanning electron microscope (SEM) (Hitachi S-2500) equipped with an EDS system for elemental analysis (Link-ISIS300 Oxford).

3. Results and Discussion

3.1 Mechanical Properties

Table 1 summarizes the components and mechanical properties of Al_2O_3, AT, and ATC composites. The relative density of the AT composite was slightly lower than the Al_2O_3 ceramic, which is due to the incorporation of TiC causing the difficulty of sintering. However, due to the existence of cobalt, the relative density of the ATC composite was the highest and its average grain size was the smallest. The melting point of cobalt is 1495 °C; under the sintering temperature, cobalt becomes fluid and can fill the pores among grains. The presence of cobalt along the grain boundary not only prevents Al_2O_3 and TiC from growing but also inhibits the reaction between Al_2O_3 and TiC during the sintering process, which usually produces a vapor phase and forms pores in the Al_2O_3-TiC series of ceramics (Ref 7). Figure 1 shows that Al_2O_3, TiC, and Co are present in the ATC composites. There is no other new phase present in the XRD spectrum, which indicates that there is no reaction during sintering process. It can be seen from Table 1 that the flexure strength and fracture toughness of the ATC composites are increased by 89.8 and 90.5% with respect to the AT composite and by 130 and 134.5% with respect to monolithic Al_2O_3, which evidences that the ATC composites have a reasonably strong interfacial bonding. Figure 2 shows the typical SEM micrographs of the fracture surfaces of the Al_2O_3, AT and ATC composites. The fracture surface of Al_2O_3 is almost completely intergranular (Fig. 2a) and that of AT is predominantly intergranular (Fig. 2b). However, the fracture surface of ATC shows a large proportion of transgranular cracks with some intergranular type (Fig. 2c).

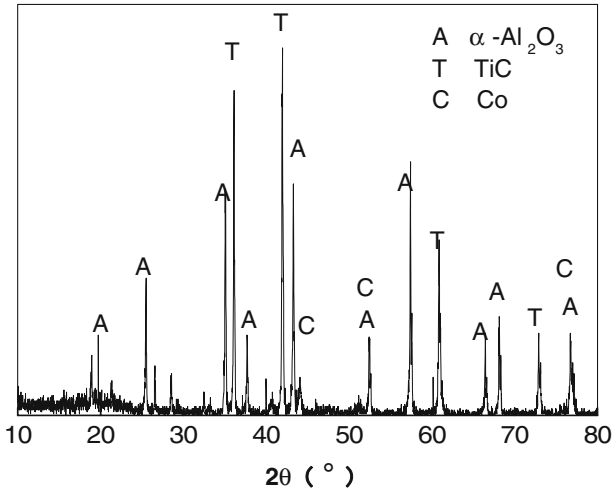

Fig. 1 x-Ray diffraction pattern of the polished surface of ATC composites

It is well known that ceramic grains are bonded by covalent and ionic forces. On the grain boundaries, neighboring grains mainly make up a 'hard' type of bonding of ceramic interface, which turns out to be the stress concentration area and a potential crack nucleation zone. Grain boundaries become the tunnels of rapid crack propagation (Ref 7). For the ATC composites, most cobalt particles residing at triple junctions (see Fig. 3) change the 'hard' type bonding of the ceramic interface, and the load can be easily transferred through the metal phase. However, ductile cobalt deforms plastically and dissipates a part of energy of crack initiation and propagation. Thus, the presence of cobalt along the grain boundary makes a great contribution to the high flexure strength of 782 ± 60 MPa and the high fracture toughness of 7.81 ± 0.80 MPa m$^{1/2}$ of the ATC composites.

3.2 Thermal Shock Properties

Figure 4 shows the effects of single thermal shock on the flexure strength of Al_2O_3, AT, and ATC composites. The retained flexure strength of the three materials decreased moderately within a certain thermal shock temperature difference ΔT, and then sharply dropped at a point corresponding to the critical thermal shock temperature difference ΔT_c, followed by a gradual decrease for further increasing temperature difference. The critical thermal shock temperature difference ΔT_c of Al_2O_3 and AT was 200 °C. With further increase in ΔT,

Table 1 Component and mechanical properties of Al_2O_3, AT and ATC composites

Material	Al_2O_3, vol.%	TiC, vol.%	Co, vol.%	Relative density, %	Average grain size, μm	Flexure strength, MPa	Fracture toughness, MPa m$^{1/2}$
Al_2O_3	100	…	…	98.9	4.1	340 ± 41	3.33 ± 0.36
AT	74.2	25.8	…	98.7	2.9	412 ± 65	4.10 ± 0.60
ATC	71.28	24.76	3.96	99.3	2.4	782 ± 60	7.81 ± 0.80

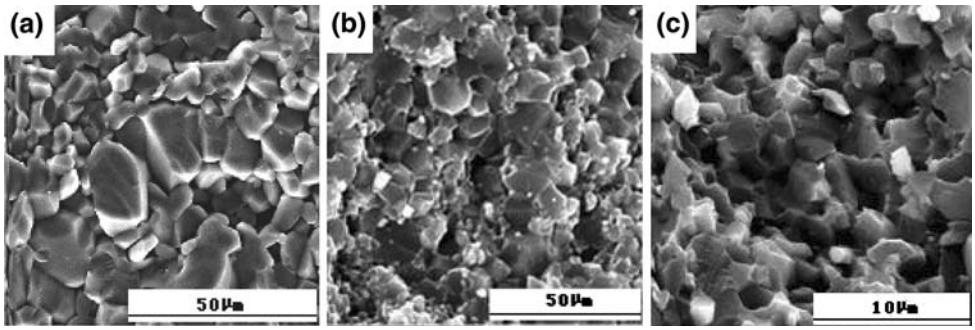

Fig. 2 SEM photographs of fracture surfaces (a) Al_2O_3, (b) AT, (c) ATC

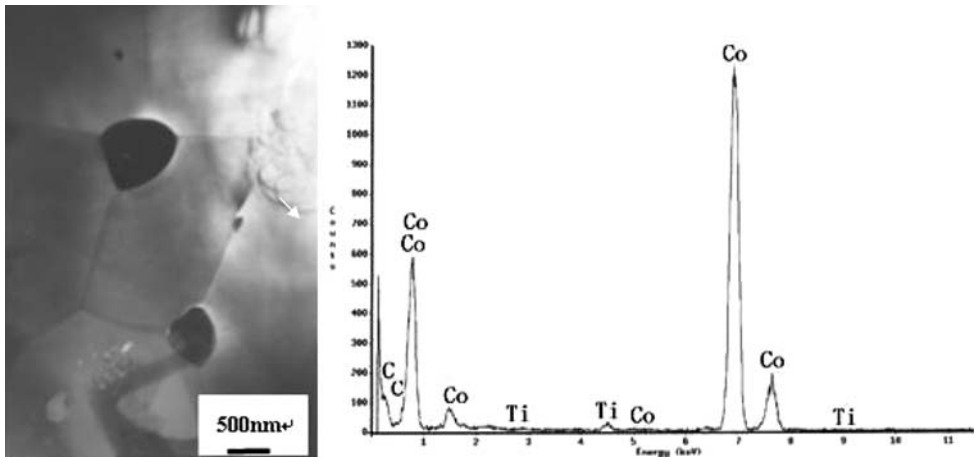

Fig. 3 TEM photograph of triple junctions grain boundary of nATC8 composite (a) and EDS pattern (b)

the retained flexure strengths of both materials decreased gradually. When thermal shock temperature difference ΔT is 600 °C the retained strengths of Al_2O_3 and AT composites dropped to 4.1 and 14.6% of their original strength, respectively. The effect of incorporating TiC into the Al_2O_3 matrix on thermal shock resistance is not evident. However, the ATC composites exhibited better resistance to crack initiation and crack propagation, possessing increased ΔT_c (about 250 °C) and higher retained strength. Especially when ΔT is increased from 600 to 800 °C, the retained strength of the ATC composite remained almost constant, while that of the AT composite dropped suddenly to 8% (ΔT = 800 °C) of its original strength. However, when ΔT was up to 1000 °C, there was a sharp drop of retained strength from 10 to 2.8%. The incorporation of a few cobalt phases into Al_2O_3-TiC composites through the powder coating technique not only improves the mechanical properties but also increases the thermal shock resistance.

Figure 5 shows SEM photographs of the fracture surface of the ATC composites after single thermal shock from 400 to 1000 °C. When ΔT is 400 °C, the grain boundaries are clear and the fracture mode is a mixture of transgranular and intergranular types. In addition, there were few isolated voids after thermal shock when ΔT is above 400 °C. The voids increased gradually with the ΔT going up. The voids were mostly isolated when ΔT is 600 °C. However, when ΔT is above 600 °C, the voids became more and larger, and most isolated voids coalesced into larger ones with the temperature going up, which caused the decrease in the density and

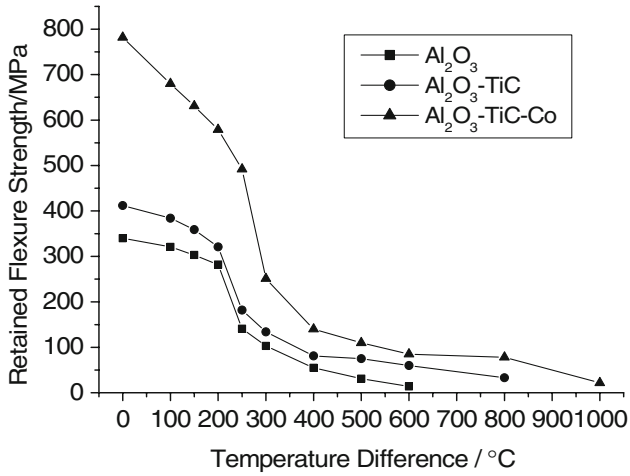

Fig. 4 Relationship between retained flexure strength and thermal shock temperature difference for the Al_2O_3, AT, and ATC composites

strength. When ΔT is increased from 600 to 800 °C, the fracture surface exhibited trace of oxidation, which was identified as Co_3O_4 by the XRD pattern. But the oxidation of TiC was not found by XRD. The oxidation reaction of Co is between the temperature range from 600 to 800 °C, which can be inferred as follows:

$$2Co + 3O_2 = 2Co_2O_3 \quad \text{(Eq 1)}$$

$$2Co + O_2 = 2CoO \quad \text{(Eq 2)}$$

$$CoO + Co_2O_3 = Co_3O_4 \quad \text{(Eq 3)}$$

With further increase to 1000 °C, intergranular fracture turns to be the primary fracture mode and the oxidation seems to be more serious together with noticeable voids interpenetration, as shown in Fig. 5d. XRD pattern (Fig. 6b) shows that TiO_2 forms after thermal shock at this temperature difference, which is usually found in Al_2O_3-TiC after heat treatment at $\Delta T = 800$ °C (Ref 8). The oxidation reaction of TiC at relatively high temperatures is expressed as follows (Ref 8):

$$TiC + 2O_2 = TiO_2 + CO_2 \uparrow \quad \text{(Eq 4)}$$

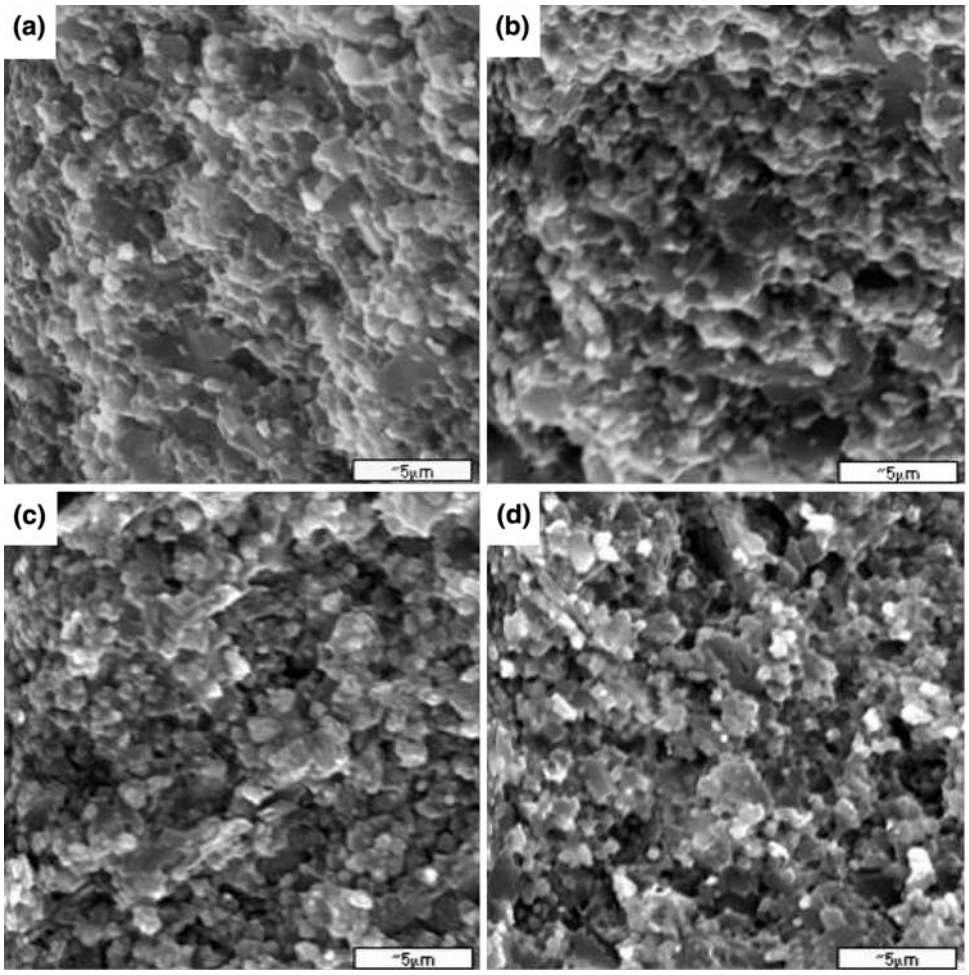

Fig. 5 SEM photographs of fracture surface of ATC composites after single thermal shock (ΔT) at: (a) 400 °C, (b) 600 °C, (c) 800 °C, and (d) 1000 °C

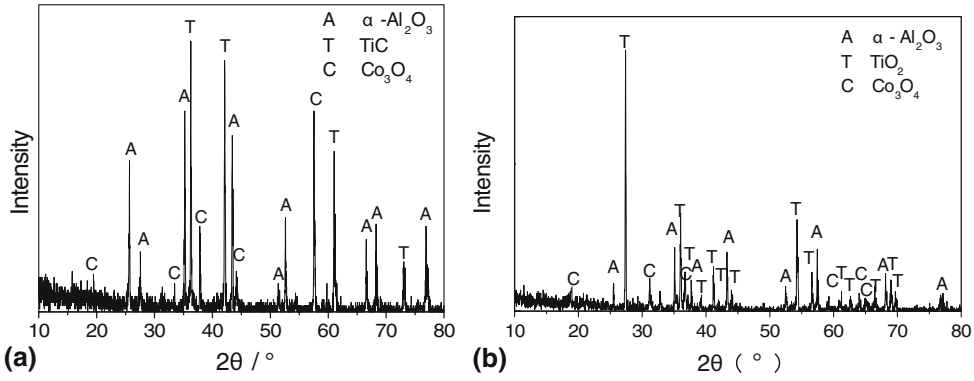

Fig. 6 x-Ray diffraction pattern of ATC composite after thermal shock (a) $\Delta T = 600$-800 °C, (b) $\Delta T = 1000$ °C

The relationship between retained flexure strength and number of thermal shock cycles of the AT and ATC composites quenched at ΔT = 400 °C is given in Fig. 7. Likewise, a higher retained strength was also obtained in the ATC composites, which indicates that the ATC composite is less sensitive to repeated thermal shock. The strength of both composites decreased initially rapidly and then tended to saturation values with increasing number of thermal shock cycles. But the retained strength of the ATC composite was higher by 72.8% than that of the AT composites after one thermal shock cycle. With increase in the thermal shock numbers above five times, the retained strength of both composites remained almost constant. The poor resistance to repeated thermal shock of the AT composites is mainly induced by stresses arising from thermal expansion mismatch between Al_2O_3 and TiC. The ductile cobalt phase between Al_2O_3 and TiC particles is assumed to relieve the thermal stresses to a degree, which should be responsible for the higher resistance to thermal shock damage. The SEM photographs of the fracture surface of the ATC composites showed that a few large voids were seen (Fig. 8a) and a few orchid-like products of oxidation could be universally found after five cycles (Fig. 8b). EDS results confirm that it is the mixture of oxides of Sodium and Titanium. With increasing cycles, the voids became larger and some voids interpenetrated after twenty times of thermal shock cycles (Fig. 8c). In addition, some leaf-like products of oxidation were found on the fracture surface after 20 cycles (Fig. 8d). EDS results certify that it is also the mixture of oxides of Sodium and

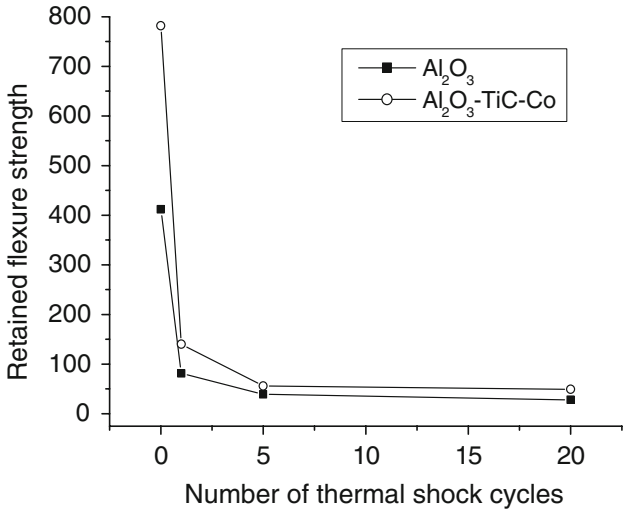

Fig. 7 Relationship between retained flexure strength and number of thermal shock cycles (ΔT = 400 °C)

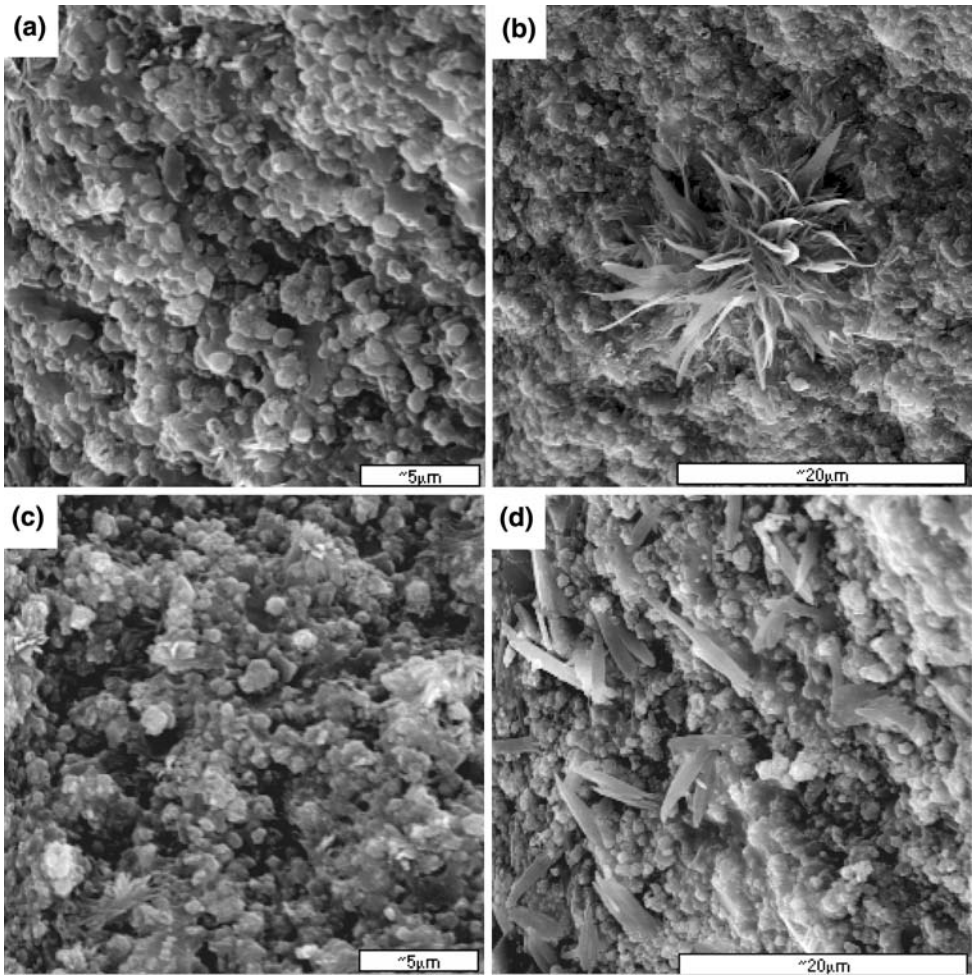

Fig. 8 SEM photographs of fracture surface of ATC composite after different quenching cycles (ΔT = 400°C) (a) and (b) 5 cycles, (c) and (d) 20 cycles

Titanium. The presence of oxide and voids impaired the continuity of body severely and degraded the retained strength of the ATC composites.

4. Conclusions

The novel Al_2O_3-TiC-Co composites containing 3.96 vol.% cobalt showed better mechanical properties and thermal shock resistance than the traditional Al_2O_3 and Al_2O_3-TiC composites. The flexure strength and fracture toughness of ATC composites are greatly improved compared with monolithic Al_2O_3 and Al_2O_3-TiC. The thermal quenching experiments indicated that the incorporation of cobalt provides beneficial contribution to both the resistance to thermal shock fracture and thermal shock damage. The ATC composites exhibited better resistance to single and repeated thermal shock. The critical temperature difference for the ATC composites (about 250 °C) was improved by about 50 °C compared with that of the AT composites (about 200 °C). This should be attributed to the enhanced strength. At any different thermal shock temperature difference, the retained strength of the ATC composite was higher than that of the AT composite. SEM photographs of the fracture surfaces of the ATC composites after single thermal shock showed that the voids became more and larger, and most isolated voids coalesced into larger ones with temperature difference going up, which caused the decrease in the density and strength. Likewise, the results of repeated thermal shock indicated that the ATC composite is less sensitive to repeated thermal shock than the AT composites.

Acknowledgment

This work was sponsored by the Doctoral Fund of Shandong Province (Grant No. 2006BS04037), National Nature Science Fund of China (Grant No. 50572034), and the primary program of University of Jinan (Y0602).

References

1. L. Wang, J.L. Shi, and J.H. Gao, Influence of Tungsten Carbide Particles on Resistance of Alumina Matrix Ceramics to Thermal Shock, *J. Eur. Ceram. Soc.*, 2001, **21**, p 1213–1217 (in English)
2. L. Wang, J.L. Shi, and Z.L. Hua, The Influence of Addition of WC Particles on Mechanical Properties of Alumina-Matrix Composite, *Mater. Lett.*, 2001, **50**, p 179–182 (in English)
3. J.H. Gong, Z. Zhao, and H.Z. Miao, R-curve Behavior of TiC Particles Reinforced Al_2O_3 Composites, *Scr. Mater.*, 2000, **43**, p 27–31 (in English)
4. X. Ai, Z.Q. Li, and J.X. Deng, Development and Perspective of Advanced Ceramic Cutting Tool Material, *Key Eng. Mater.*, 2001, **96**, p 98–112 (in English)
5. C.H. Xu, X. Ai, and C.Z. Huang, Fabrication and Performance of an Advanced Ceramic Tool Material, *Wear*, 2001, **249**, p 503–508 (in English)
6. X.M. Shi, Y.B. Pan, and J.K. Guo, Fabrication and Magnetic Properties of Cobalt-Dispersed-Alumina Composite, *Ceram. Int.*, 2007, **33**, p 1509–1513 (in English)
7. J. Li, J.L. Sun, and L.P. Huang, Effects of Ductile Cobalt on Fracture Behavior of Al_2O_3-TiC, *Mater. Sci. Eng.*, 2002, **A323**, p 17–20 (in English)
8. L.H. Zhang and R.V. Koka, A Study on the Oxidation and Carbon Diffusion of TiC in Alumina-Titanium Carbide Ceramics Using XPS and Raman Spectroscopy, *Mater. Chem. Phys.*, 1998, **57**(1), p 23–32 (in English)